

$b=0$:

$$v_p = [\alpha_I (x_s - x) - l/\theta_w]^{-1} \quad (11a)$$

$$y = x_s (\theta_s - \theta_w) - \alpha_I^{-1} l_w [l + \alpha_I \theta_w (x - x_s)] \quad (11b)$$

$$\rho_p = \{l - \theta_w/\theta_s + \theta_s^{-1} [\alpha_I (x - x_s) + l/\theta_w]^{-1}\}^{-1} \quad (11c)$$

Discussion

1) The results for u_p , v_p , and y are equivalent to those of Peddieson and Lyu.² The expression for T_p is also equivalent, but our result is in a much simpler form and does not depend explicitly on the drag law used (i.e., the value of b).

2) When $b=3/5$, our result for ρ_p is equivalent to the result of Peddieson and Lyu. However, when $b=1$, their result for ρ_p should read

$$\rho_p = [l - (\alpha_I/\theta_s) (z_s - z)]^{-1}$$

and when $b=0$, their result for ρ_p should be

$$\rho_p = [l - (\theta_w/\theta_s) \{l - \exp[\alpha_I (z - z_s)]\}]^{-1}$$

These corrected results are then equivalent to our results (9c) and (11c), respectively.

3) We note that for all values of b ,

$$\rho_p \rightarrow \theta_s / (\theta_s - \theta_w) = l/\epsilon \text{ as } x \rightarrow \infty$$

where ϵ is the gas density ratio across the shock. The results of Peddieson and Lyu incorrectly indicate that $\rho_p \rightarrow \infty$ as $x \rightarrow \infty$.

4) For $b=0$, all particles strike the wedge, since $y>0$ for all x_s as $x \rightarrow \infty$. However, for $b=1$, particles will not strike the wedge if $x_s > \theta_w / [\alpha_I (\theta_s - \theta_w)]$, and for $b=3/5$, particles will not strike the wedge if $x_s > 5\theta_w^{3/5} / [3\alpha_I (\theta_s - \theta_w)]$.

Acknowledgment

This work was supported by National Research Council of Canada under Grant No. A4484.

References

- ¹ Probst, R. F. and Fassio, F., "Dusty Hypersonic Flows," *AIAA Journal*, Vol. 8, No. 4, April 1970, pp. 772-779.
- ² Peddieson, J. and Lyu, C-H., "Dusty Hypersonic Wedge Flows," *AIAA Journal*, Vol. 11, No. 1, Jan. 1973, pp. 110-112.

Shape Factors between Coaxial Annular Disks Separated by a Solid Cylinder

C. P. Minning*

Hughes Aircraft Co., Culver City, Calif.

Nomenclature

x, y, z = Cartesian coordinates of dA_I , cm
 l_1, m_1, n_1 = cosines (i.e., direction cosines) of the angles between the normal to dA_I and the x, y , and z axes, respectively

Received Sept. 19, 1978. Copyright © American Institute of Aeronautics and Astronautics, Inc., 1978. All rights reserved.

Index categories: Radiation and Radiative Heat Transfer; Thermal Modeling and Analysis; Spacecraft Temperature Control.

*Staff Engineer, Electro-Optical and Data Systems Group.

x_2, y_2, z_2 = Cartesian coordinates of a point on the periphery of surface 2, cm
 S = distance between dA_I and a point on the periphery of surface 2, cm
 r = radial coordinate in plane of surface 2, cm
 r_o, r_i = outer and inner radii, respectively, of surface 2, cm
 r_c = radius of cylinder, cm
 ρ = radial coordinate in plane of dA_I , cm
 θ = angular displacement from x axis, rad
 ϵ = emissivity
 ϕ, ω = viewing angles, rad
 h = vertical distance between surface 1 and surface 2, cm

Introduction

THE calculation of shape factors between parallel, coaxial annular disks with identical radii separated by a solid coaxial cylinder having the same radius as the inner radii of the disks is a relatively easy task which can be performed with the aid of shape-factor algebra and the closed-form expressions given in Hamilton and Morgan.¹ However, this is not the case when it is necessary to evaluate the shape factors between disks with different radii. This latter geometry, for which there is no closed-form expression available in the literature, is oftentimes encountered in thermal control calculations for spin-stabilized spacecraft and in discrete-element thermal models for annular fin-tube radiators for spacecraft applications.

In their analysis of annular fin-tube radiators, Sparrow et al.² used the contour integration method³ to evaluate the radial dependence of shape factors between differential areas on opposing fins. However, this analysis, which required the numerical solution of a nonlinear, integro-differential equation for the temperature distribution in a fin, was carried out only for black ($\epsilon=1$) surfaces and no incident radiation from external sources (i.e., direct solar, albedo, and Earth IR). Since any realistic, spacecraft radiator design must account for nonblack ($\epsilon<1$) surfaces and external radiant heating, the most convenient method for analyzing such a system requires the formulation of a discrete-element thermal model in which each fin is divided up into a number of finite annular segments. Thus, it is necessary to evaluate the shape factors between the annular segments of the opposing fins.

The contour integral method is used in the present analysis to derive a closed-form expression for the shape factor from a differential area on one fin to a finite-sized annular area on the opposing fin. This expression can then be integrated numerically to obtain the desired shape factors between finite-sized annular areas on opposing fins. Results are given for some typical fin-tube geometries.

Analysis

Consider the geometry shown in Figs. 1 and 2 which illustrate the nomenclature used in this presentation. Throughout this discussion, surface 2 is always considered to be of finite size; surface 1 can be either a differential area or a finite-sized area, depending on the problem under consideration.

Sparrow³ has shown that $F_{dA_I-A_2}$ can be expressed as the sum of three contour integrals in the following manner:

$$F_{dA_I-A_2} = l_1 \oint_C \frac{(z_2 - z) dy_2 - (y_2 - y) dz_2}{2\pi S^2} + m_1 \oint_C \frac{(x_2 - x) dz_2 - (z_2 - z) dx_2}{2\pi S^2} + n_1 \oint_C \frac{(y_2 - y) dx_2 - (x_2 - x) dy_2}{2\pi S^2} \quad (1)$$

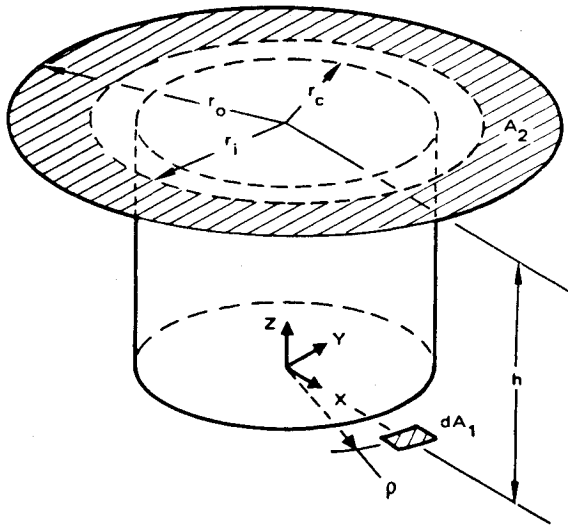


Fig. 1 Nomenclature for shape factor from a differential area to a disk, the view of which (as seen from dA_1) is partially blocked by a solid coaxial cylinder.

where

$$S^2 = (x_2 - x)^2 + (y_2 - y)^2 + (z_2 - z)^2 \quad (2)$$

Here, the letter C designates integration around the periphery of surface 2. Since the normal to dA_1 is parallel to the z axis, $l_1 = m_1 = 0$, and $n_1 = 1$. Hence, only the last term in Eq. (1) is nonzero.

Integration around the periphery of surface 2 is performed in the clockwise direction in four steps, each step corresponding to one of the numbered boundaries shown in Fig. 2. For boundary 1: $x_2 = r_o \cos \theta$, $dx_2 = -r_o \sin \theta d\theta$, $y_2 = r_o \sin \theta$, $dy_2 = r_o \cos \theta d\theta$, and $z_2 = h$. For boundary 3: $x_2 = r_i \cos \theta$, $dx_2 = -r_i \sin \theta d\theta$, $y_2 = r_i \sin \theta$, $dy_2 = r_i \cos \theta d\theta$, and $z_2 = h$. The contour integrals along boundaries 2 and 4 are equal to zero (see discussion in Ref. 2, p. 1294). For all boundaries, $x = \rho$, $z = 0$, and $y = 0$. The visible portion of A_2 , as seen from dA_1 , is defined by the view angles ω and ϕ , which are defined as follows (see Fig. 2):

$$\omega = \cos^{-1}(r_c/\rho) + \cos^{-1}(r_c/r_o) \quad (3)$$

$$\phi = \cos^{-1}(r_c/\rho) + \cos^{-1}(r_c/r_i) \quad (4)$$

Substitution of the appropriate expressions for x, y, x_2 , and y_2 into Eq. (1) results in the following:

$$F_{dA_1-A_2} = -\frac{r_o}{2\pi} \int_{+\omega}^{-\omega} \frac{(r_o - \rho \cos \theta) d\theta}{r_o^2 + \rho^2 + h^2 - 2\rho r_o \cos \theta} - \frac{r_i}{2\pi} \int_{-\phi}^{+\phi} \frac{(r_i - \rho \cos \theta) d\theta}{r_i^2 + \rho^2 + h^2 - 2\rho r_i \cos \theta} \quad (5)$$

The integrals in this expression are available in standard references.⁴ The desired equation for $F_{dA_1-A_2}$ is then found to be

$$F_{dA_1-A_2} = \frac{\omega - \phi}{2\pi} + \frac{(r_o^2 - \rho^2 - h^2)}{\pi \sqrt{(r_o^2 + \rho^2 + h^2)^2 - 4\rho^2 r_o^2}} \tan^{-1} \left[\sqrt{\frac{r_o^2 + \rho^2 + h^2 - 2\rho r_o}{r_o^2 + \rho^2 + h^2 + 2\rho r_o}} \tan \frac{\omega}{2} \right] \\ - \frac{(r_i^2 - \rho^2 - h^2)}{\pi \sqrt{(r_i^2 + \rho^2 + h^2)^2 - 4\rho^2 r_i^2}} \tan^{-1} \left[\sqrt{\frac{r_i^2 + \rho^2 + h^2 - 2\rho r_i}{r_i^2 + \rho^2 + h^2 + 2\rho r_i}} \tan \frac{\phi}{2} \right] \quad (6)$$

Consider the special case where $r_i = r_c = 0$. For this situation, $\omega = \phi = \pi$, and Eq. (6) reduces to

$$F_{dA_1-A_2} = \frac{1}{2} \left[1 + \frac{r_o^2 - \rho^2 - h^2}{\sqrt{(r_o^2 + \rho^2 + h^2)^2 - 4\rho^2 r_o^2}} \right] \quad (7)$$

which is the familiar expression for the shape factor between an off-center differential area to an unblocked circular disk.

Now consider the special case where $\rho = r_i = r_c$, where $r_c \neq 0$. For this situation, Eq. (6) reduces to

$$F_{dA_1-A_2} = \frac{\omega}{2\pi} + \frac{(r_o^2 - \rho^2 - h^2)}{\pi \sqrt{(r_o^2 + \rho^2 + h^2)^2 - 4\rho^2 r_o^2}} \tan^{-1} \left[\sqrt{\frac{r_o^2 + \rho^2 + h^2 - 2\rho r_o}{r_o^2 + \rho^2 + h^2 + 2\rho r_o}} \tan \frac{\omega}{2} \right] \quad (8)$$

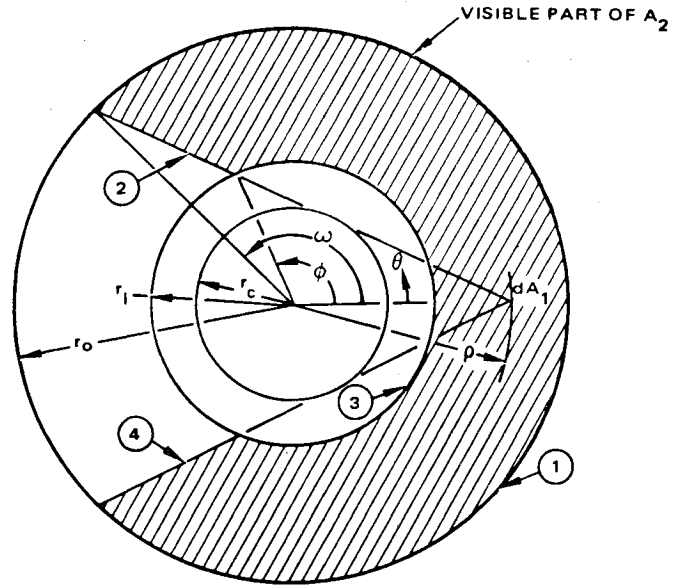


Fig. 2 The visible portion of the finite-sized disk, A_2 , as seen from the differential area dA_1 .

Equation (15d) of Ref. 3 reduces to the above expression for $R_1 = R_2 \cos \theta_o$ (R_1, R_2, θ_o are Ref. 3 nomenclature).[†]

Shape factors from a differential area to a partially blocked disk (inner radius $= r_c$) are plotted against ρ/r_c , for several values of r_o/r_c , in Fig. 3. It is seen that the shape factor at first increases, passes through a maximum, and then decreases as ρ is increased from r_c . These curves can be used, along with shape-factor algebra, to calculate the shape factors from dA_1 to any disk having an inner radius in the range $r_c \leq r_i < r_o$.

Shape factors between finite-sized disk segments can be determined by integrating Eq. (6) in the following manner:

$$F_{A_1-A_2} = \frac{2}{(\rho_o^2 - \rho_i^2)} \int_{\rho_i}^{\rho_o} \rho F_{dA_1-A_2} d\rho \quad (9)$$

[†]Note that a minus sign should precede λ^2 in the expression enclosed by parentheses in the second term of Eq. (15d), Ref. 3.

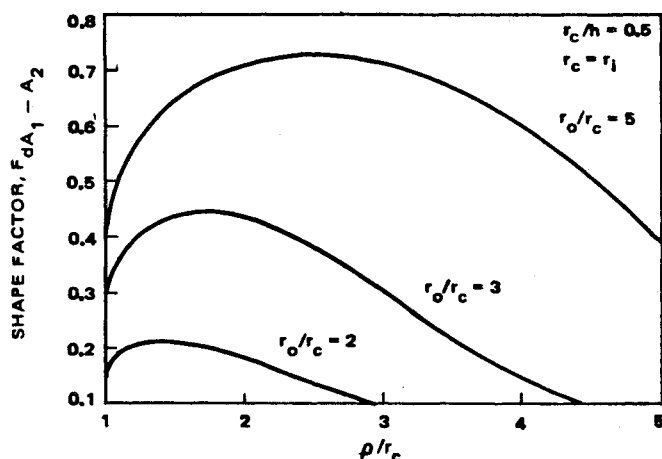


Fig. 3 Shape factor from a differential area to a disk, the view of which (as seen from dA_1) is partially blocked by a solid cylinder ($r_c/h=0.5$, $r_c=r_i$).

Despite the comparatively simple form of Eq. (6), the evaluation of Eq. (9) in closed form is, at best, difficult. Therefore, Eq. (9) was evaluated numerically, and some typical results are shown in Fig. 4. Note that for $r_c=r_i=\rho_i$ and $r_o=r_o$, the results are identical to these given for configurations A7 and A8 in Ref. 1.

Acknowledgment

This paper is based on work performed under the sponsorship of Comsat General Corporation. Any views expressed in this paper will not necessarily be those of Comsat General.

References

- ¹Hamilton, D.C. and Morgan, W. R., "Radiant-Interchange Configuration Factors," NACA TN 2836, 1952, pp. 37, 42.
- ²Sparrow, E. M., Miller, G. B., and Jonsson, V. K., "Radiating Effectiveness of Annular-Finned Space Radiators, Including Mutual

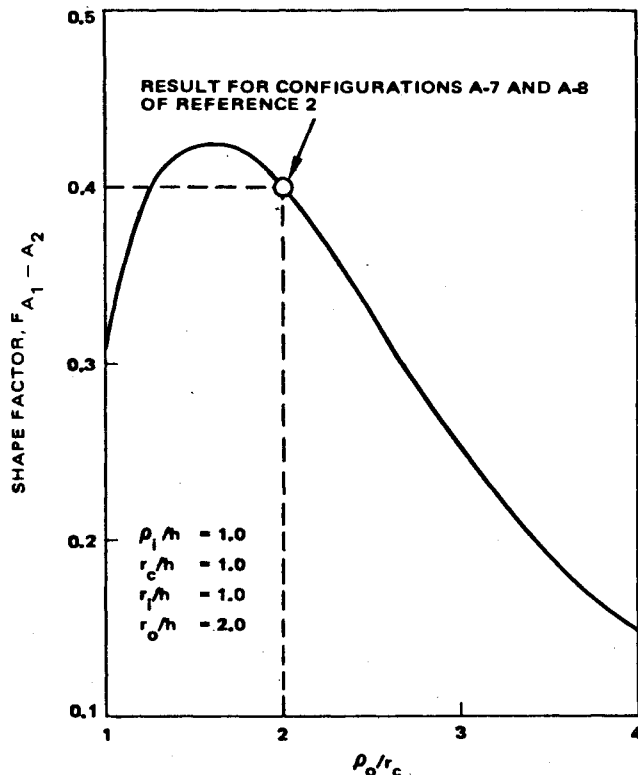


Fig. 4 Shape factor $F_{A_1-A_2}$, between finite-sized coaxial disks separated by a solid cylinder ($\rho_i/h=r_c/h=r_i/h=1.0$, $r_o/h=2.0$).

Irradiation Between Radiator Elements," *Journal of Aerospace Science*, Vol. 29, Nov. 1962, pp. 1291-1299.

³Sparrow, E. M., "A New and Simpler Formulation for Radiative Angle Factors," *Journal of Heat Transfer, Transactions of ASME, Ser. C*, Vol. 85, Feb. 1963, pp. 81-88.

⁴Gradshteyn, I. S. and Ryzhik, I. M., *Table of Integrals, Series, and Products*, 4th ed., translated and edited by Alan Jeffrey, Academic Press, New York, 1965, pp. 68, 148.